Accepted Manuscript

Why is *cis*/*trans* stereoinversion with $Li^{+}(THF)_4$ migration across the phenyl ring of α-lithiostyrene *accelerated* by two *ortho*-methyl groups?

Rudolf Knorr, Ernst Lattke, Jakob Ruhdorfer, Kathrin Ferchland, Ulrich von Roman

PII: S0040-4020(18)30107-8

DOI: 10.1016/j.tet.2018.01.047

Reference: TET 29262

To appear in: *Tetrahedron*

Received Date: 11 October 2017

Revised Date: 24 January 2018

Accepted Date: 26 January 2018

Please cite this article as: Knorr R, Lattke E, Ruhdorfer J, Ferchland K, von Roman U, Why is *cis*/*trans* stereoinversion with $Li^{+}(THF)_4$ migration across the phenyl ring of α-lithiostyrene *accelerated* by two *ortho*-methyl groups?, *Tetrahedron* (2018), doi: 10.1016/j.tet.2018.01.047.

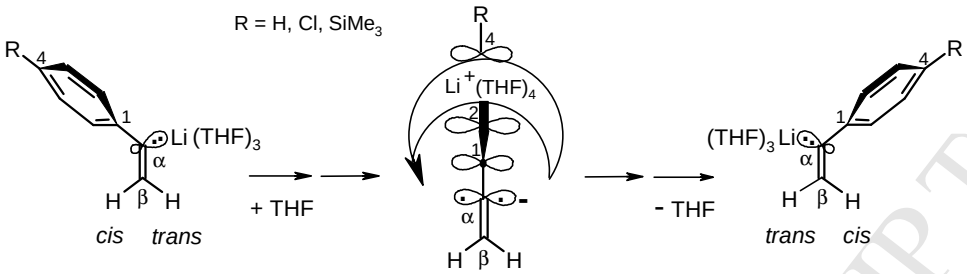

Why is *cis*/*trans* stereoinversion with $Li^+(THF)_4$ migration across the phenyl ring of α-lithiostyrene *accelerated* by two *ortho*-methyl groups?

In memory of Professor Joseph Klein

Rudolf Knorr, Ernst Lattke, Jakob Ruhdorfer, Kathrin Ferchland, Ulrich von Roman

ABSTRACT

Common wisdom might anticipate that two methyl groups placed on a molecular migration route should act as an impediment. However, the "conducted tour" migration of $Li^+(THF)_4$ across the aryl ring ("π-route") during the *cis*/*trans* stereoinversion of α-arylvinyllithiums had been found to occur with practically equal velocities in the presence of either one or two *ortho*-alkyl substituents. We now report that the omission of both *ortho*-methyl groups *retards* the stereoinversion process. In order to arrive at an answer to the title question, we investigate the aggregation equilibria and microsolvation states of *ortho,ortho´*-unsubstituted α-lithiostyrenes by means of approved secondary NMR criteria. Beyond such necessary knowledge about the ground-state properties, we provide kinetic evidence showing that the retarded *cis*/*trans* stereoinversion of α-lithiostyrene proceeds by the pseudomonomolecular, ionic mechanism with $Li^+(THF)_4$ migration.

Key words: Aggregation, Li^+ migration, Microsolvation, Reaction mechanisms, Stereolability, Vinylanions

1. Introduction

Crystallographic studies of many organolithium compounds disclosed a multitude of solid-state structures with various kinds of aggregation and degrees of microsolvation (namely, the coordination of "explicit" electron-pair donating ligands at lithium).[1–5] These structures may or may not survive a transfer from the crystal into a solution; therefore, dissolved organolithiums require additional analytic techniques for differentiating monomeric from dimeric and higher aggregational states. Under suitable conditions, scalar NMR one-bond coupling constants $^1J(^{13}C,^6Li)$ or (less conveniently) $^1J(^{13}C,^7Li)$ can provide such differentiations. In contrast to molecular weight determinations, this NMR technique can work even for contaminated solutions and in the presence of two or more organolithium species.[6] Due to the high mobility of Li^+ cations within and between dissolved organolithium molecules, however, such $^{13}C,^6Li$ spin-spin coupling must be sought at sufficiently low temperatures that retard intermolecular Li^+ scrambling and conserve $^6Li–^{13}C(\alpha)$ spin

coherence on the NMR time scales. Since the most common monodentate (nonchelating) ligands such as tetrahydrofuran (THF) or Et_2O often are even more mobile than Li^+, determinations of their microsolvation numbers *d* in solution remained difficult for a long time. Scheme 1 displays α-arylalkenyllithiums **1** – **12** whose (non)aggregation and microsolvation states were established[7–15] through the above $^1J_{C,Li}$ technique: With one exception[15] (namely, dimeric **10**), all of these compounds turned out to be monomeric in THF as the solvent; all of these monomers were trisolvated with *d* = 3 THF ligands at Li^+. With non-THF ligands such as Et_2O or *tert*-butyl methyl ether (*t*-BuOMe), the monomeric species of **1a**–**e**,[7] **5c**,[13] and **7b**[13] were only disolvated (*d* = 2), whereas most of the other examples in Scheme 1 formed disolvated dimers with *d* = 1 monodentate ligand at Li. Steric congestion by bulky substituents in the C-β region of **1a**–**e** or at the *ortho*,*ortho´*-positions of the α-aryl group (**5c**, **7b**) disfavored dimerization of the monomers. Higher aggregated states were detected for unsolvated species (*d* = 0) of **1a**, **5c**, and **10**–**12** that were sufficiently soluble in donor-free hydrocarbon solvents; however, only the unsolvated cyclotrimeric[7] species of **1a** could be structurally characterized.

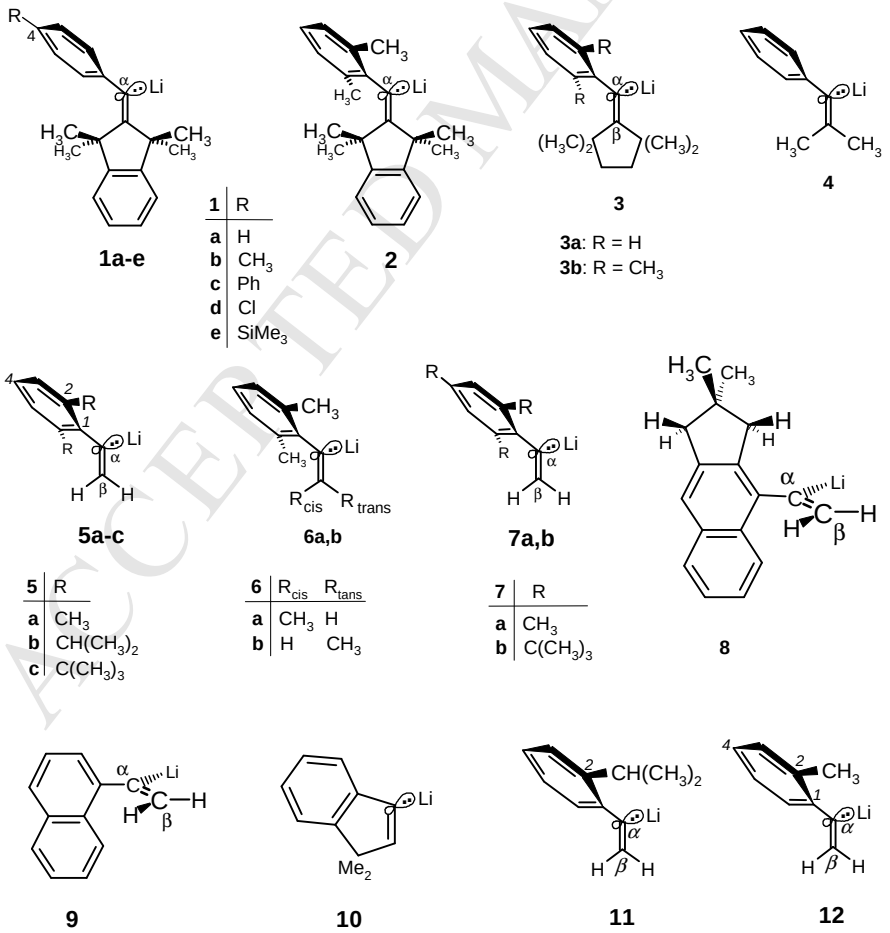

Scheme 1 α-Arylalkenyllithiums whose (non)aggregation and microsolvation states had been established in solution: **1a**–**e**,[7,8] **2**,[8] **3**,[9] **4**,[10] **5a**,[11] **5b**,[12] **5c**,[13] **6a** and **b**,[10] **7a**,[11] **7b**,[13] **8**,[14] **9**,[14] and **10**–**12**.[15]

The most direct experimental evidence for the discrete microsolvation numbers d = 1 or 2 at Li was obtained through NMR integration only from the sterically congested α-arylalkenyllithiums **1a**,[7] **1e**,[8] **3a**,[9] and **5b**,[12] whose ligand scrambling was sufficiently retarded: The ^{1}H and ^{13}C NMR spectra of **5b** displayed separate signals for free and coordinated (immobilized) monodentate ligands, so that the d values followed from the NMR integrals of the immobilized ligands in comparison with suitable integrals of the carbanionic part. These integral ratios and also the magnitudes of the above $^{1}J_{C,Li}$ couplings[7] were dubbed primary NMR criteria of microsolvation; but such criteria are unavailable without steric shielding and efficient cooling of the solutions. Therefore, the less encumbered examples in Scheme 1 had to be analyzed by secondary NMR criteria: First, scalar two-bond coupling constants $^{2}J_{H,H}$ between the two β-protons in the H_2C=C moieties can reveal microsolvation numbers.[11] Second, chemical shift differences $\Delta\delta$ between corresponding nuclei of an organolithium (RLi) and its "parent" substance (RH) can also serve as secondary criteria: Some of these lithiation shifts $\Delta\delta = \delta$(RLi) – δ(RH) may contain hints at microsolvation, aggregation, and the α-aryl conformation. Except for **10** whose α-aryl group is conformationally fixed, all other compounds in Scheme 1 preferred a close to perpendicular relationship of the α-aryl and the C(α)=C(β) double-bond planes; even the single small 2-CH_3 substituent in **12** did not admit greater deviations from this conformation that is preserved by substantial electronic barriers[12,14] against α-aryl rotation about the C(α)–C(1) bond. Considering that the above conformational preference and the resistance against aggregation in THF had been detected also for all three α-arylvinyllithiums (**9**, **11**, and **12**) that carry only one *ortho*-substituent, we felt motivated to extend earlier studies[16] of examples without any *ortho* substituent, in particular to the apparently "simple" α-lithiostyrene. The present kinetic results raised the title question and provided an answer that is compatible with the "conducted tour"[14] migration.

2. Results and discussion

2.1. Preparation, ground states, and aggregation of the o,o´-unsubstituted α-lithiostyrenes

The Br/Li interchange reaction (Scheme 2) of α-bromo-4-(trimethylsilyl)styrene (**13a**) with *n*-butyllithium (*n*-BuLi, 1.1 equiv) to give α-[4-(trimethylsilyl)phenyl]vinyllithium (**14a**) and 1-bromobutane (*n*-BuBr) was surprisingly fast in donor-free pentane as the solvent: Unsolvated **14a** emerged with a first half-reaction time of ca. 8 min at 32 °C and displayed a considerably broadened AB-type spectrum of its β-protons with $^{2}J_{H,H}$ = 4.0 Hz. Regrettably, this donor-free species of **14a** began to decay with polymerization. In Et_2O as the solvent, the Br/Li interchange of **13a** was much faster and furnished the Et_2O-solvated species of **14a** that

polymerized less rapidly and formed the acid **16a** on carboxylation with solid CO_2; however, the interfering reaction of **14a** with its coproduct *n*-BuBr started soon and was complete within two days at room temperature (rt). In order to prevent such a destruction of **14a**, *n*-BuBr and all other volatile impurities were removed from the Et_2O solution under reduced pressure (< 0.1 mbar), leaving **14a** together with some LiBr (ca. 0.3 equiv) as an oily residue that was dissolved in Et_2O, THF, or other anhydrous solvents for the NMR studies. Since the above-mentioned primary NMR criterion of $^{13}C,^{6}Li$ spin-spin coupling remained unavailable for **14a** and for all of the following *ortho*-unsubstituted α-lithiostyrenes even at the lowest temperatures, we used the secondary NMR criteria of lithiation shifts, $\Delta\delta = \delta(\text{RLi}) - \delta(\text{RH})$, as a tool for purging δ(RLi) from some of the constitutional effects that are also present in δ(RH).

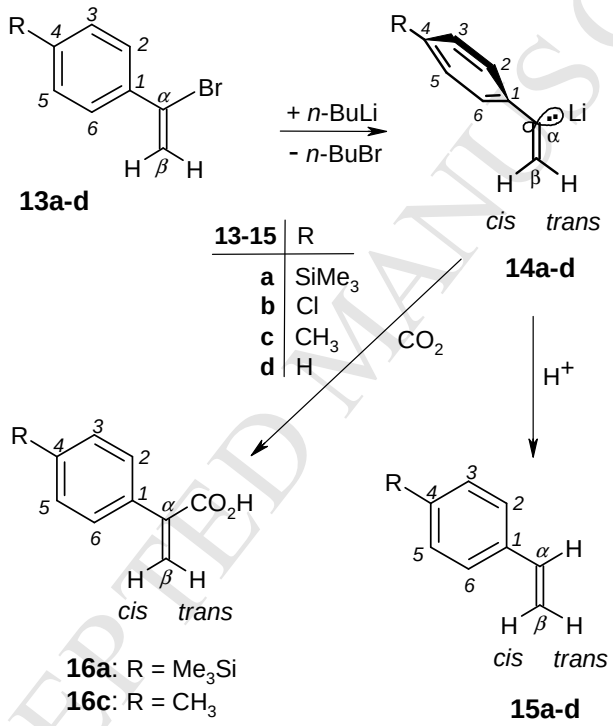

Scheme 2. Preparation and derivatization of the α-arylvinyllithiums **14a**–**d**.

In Et_2O as the solvent at 25 °C, the value of $\Delta\delta$(C-1) = +20.7 ppm (entry 6 of Table 1) classified **14a** as predominantly dimeric on account of the similar values of the established dimers of **5a** (entry 2)[11] and **12** (entry 4).[15] The strongly positive $\Delta\delta$(C-β) in entry 6 will turn out to be characteristic of the other dimeric **14** fellows; but **14a** was not sufficiently stable to furnish additional evidence at and below rt. On the other hand, **14a** was stable in THF as the solvent in the absence of *n*-BuBr: Its $\Delta\delta$ data for C-α, C-1, and C4 (entry 5) disclosed a nonaggregated (monomeric) state through comparison with the established monomers of **5a** (entry 1)[11] and **12** (entry 3).[15] The most strongly negative value of $\Delta\delta$(C-4) = –14.8 ppm (entry 5) is typical for Me_3Si substitution (–17.9 ppm in **1e**)[7] and due to a close to

perpendicular relationship of the α-aryl plane with respect to the C(α)=C(β) double-bond plane.[15] Although a dimeric species of **14a** could not be separately identified in this THF solution, its growing population on warming (the usual[17] endothermic dimerization) appeared to be the reason behind the temperature-dependent ^{1}H and ^{13}C NMR spectra (Tables S1[18]): The $\Delta\delta$ data became less positive for C-α and C-1 but more positive for C-β, C-4, 2-/6-H, 3-/5-H, and the two β-H resonances. The full $\Delta\delta$ set of monomeric **14a** at –115 °C is depicted in Figure 1b.

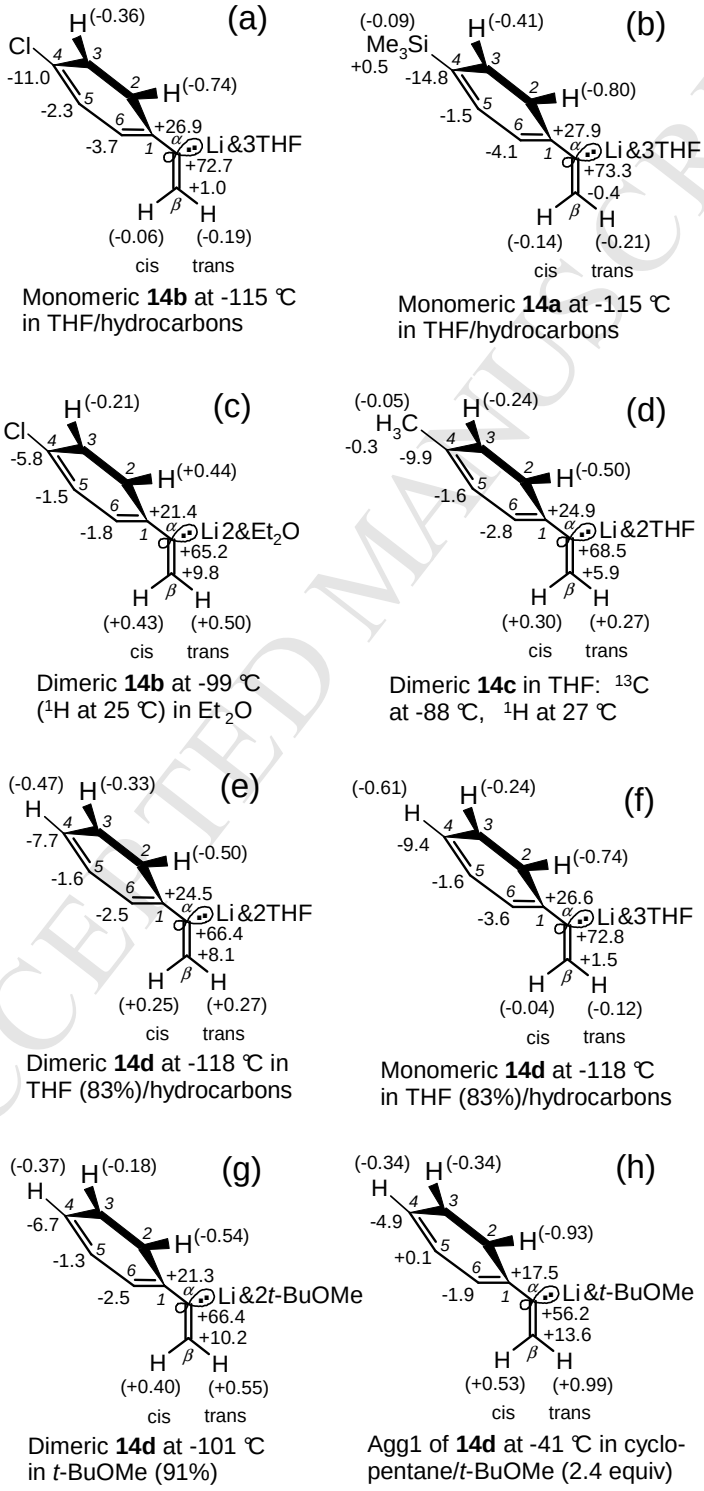

Fig. 1. Lithiation ^{1}H (in parentheses) and ^{13}C NMR shifts $\Delta\delta = \delta(\text{RLi}) - \delta(\text{RH})$ of **14a**–**d**.

Table 1. Microsolvation numbers *d*, NMR coupling constants $^2J_{H,H}$ [Hz] of CH_2-β, and lithiation shifts $\Delta\delta = \delta(\text{RLi}) - \delta(\text{RH})$ of the α-arylvinyllithiums **5a**, **12**, and **14a–d** in four solvents.

entry no.	cpd. no.	α-aryl substituent	solvent	agg [a]	$^2J_{H,H}$ [Hz] (at °C) [b]	$\Delta^2J_{H,H}$ [Hz]	*d* [c]	chemical shifts δ [ppm]					temp. °C [d]	Ref.
								C-α	C-β	C-1	C-4	4-H		
1	**5a**	2,6-Me_2	THF	M	8.8 (≤ +2)	6.6	2.9	+76.4	–10.9	+24.2	–11.0	–0.76	–89	11
2	**5a**	2,6-Me_2	*t*-BuOMe	D	5.7 (≤ –7)	3.5	1.1	+68.1	–3.6	+19.4	–7.0	–0.43	–40	11
3	**12**	2-Me	THF	M	8.0 (+25)	6.24	2.7	+77.3	–4.7	+27.8	–10.4	–0.61	–38	15
4	**12**	2-Me	Et_2O	D	–	–	–	+67.9	+5.0	+21.8	–6.1	–	–70	15
5	**14a**	4-$SiMe_3$	THF [e]	M	8.0 (≥ –50)	7.0	3.2	+73.3	–0.4	+27.9	–14.8	–	–115	f
6	**14a**	4-$SiMe_3$	Et_2O	D	5.5 (+25)	4.5	1.7	–	+9.4	+20.7	–	–	+25	f
7	**14b**	4-Cl	THF [e]	M	8.0 (–44)	7.1	3.2	+72.7	+1.0	+26.9	–11.0	–	–115	f
8	**14b**	4-Cl	Et_2O	D	5.8 (+25)	4.9	1.9	+65.2	+9.8	+21.4	–5.8	–	–99	f
9	**14c**	4-Me	THF	D	6.7 (+51)	5.6	2.3	+68.5	+5.9	+24.9	–9.9	–	–88	f
10	**14d**	4-H	THF [e]	M	–	–	–	+73.4	+1.5	+26.6	–9.4	–0.61	–118	f
11	**14d**	4-H	THF [e]	D	–	–	–	+67.7	+8.1	+24.5	–7.7	–0.47	–118	f
12	**14d**	4-H	*t*-BuOMe	D [g]	5.8 (≥ –22)	4.7	1.8	+66.4	+10.2	+21.3	–6.7	–0.37	–101	f
13	**14d**	4-H	C_5H_{10} [h]	Agg1	4.8 (+25)	3.7	1.2	+56.2	+13.6	+17.5	–4.9	–0.34	–41	f

[a] "M" = monomer, "D" = dimer at the temperatures denoted before the last column. [b] Temperatures of this $^2J_{H,H}$ value. [c] Formal value as calculated from eq 2 before rounding. [d] Temperature of determinations of $\Delta\delta = \delta(\text{RLi}) - \delta(\text{RH})$. [e] With hydrocarbon cosolvents. [f] This work. [g] Accompanied by the unidentified aggregates Agg1 and Agg2. [h] C_5H_{10} = cyclopentanewith *t*-BuOMe (2.4 equiv with respect to **14d**).

α-(4-Chlorophenyl)vinyllithium (**14b**) was prepared from bromoalkene **13b** in pentane under the above conditions (as for **14a**) with a comparably short first half-reaction time and again $^{2}J_{H,H}$ = ca. 4 Hz. In a similar race against polymerization, the procedure for **14a** was used to create **14b** and LiBr (ca. 0.3–1.4 equiv) in Et_2O solutions with subsequent evaporation of *n*-BuBr. Although the interference by polymerization reduced the number of interpretable NMR spectra drastically, the $\Delta\delta$ data (entry 7 and Figure 1a) revealed **14b** to be monomeric in THF, as shown by the similar data of monomeric **14a** in entry 5 and Figure 1b. In Et_2O as the solvent, **14b** was predominantly dimeric (entry 8 and Figure 1c), as recognized through comparisons with the established dimers of **5a** (entry 2) and **12** (entry 4). The constitutions of **14b** and **14a** in Et_2O before evaporation were confirmed through their clean addition reactions to dialkyl ketones: ^{1}H and ^{13}C NMR analyses of the pure adducts (**S8**–**S10**)[18] showed no signs of internal overcrowding. Nevertheless, *t*-Bu_2C=O added to both **14a** and **14b** only in the absence of the more reactive diisopropyl ketone, in analogy with a corresponding selectivity reported[19] for **5a**.

Unsolvated α-(4-methylphenyl)vinyllithium (**14c**) was obtained from bromoalkene **13c** with *n*-BuLi in pentane by a Br/Li interchange reaction that was complete after 60 min at rt. The precipitation of powdery **14c** was accompanied by the formation of LiBr that could not totally be removed through subsequent washings with pentane. Formation of the acid **16c**[18] through carboxylation established the constitution of **14c**. In THF as the solvent, **14c** was dimeric down to –88 °C, as revealed by Figure 1d and the following comparisons with dimeric **14b** and with the established[15] dimer of **12** in Et_2O: In the vicinity of the Li–C(α) bonds, the $\Delta\delta$(C-α) and $\Delta\delta$(C-β) values were similar for all three compounds (entries 9, 8, and 4, respectively). Thus, **14c** had overcome the usual tendency of THF to deaggregate our dimers, presumably because the π-electron-repellent 4-CH_3 disfavored the nonobserved monomer.

α-Lithiostyrene (α-phenylvinyllithium, **14d**) was prepared from α-bromostyrene (**13d**) in cyclopentane or pentane by the above procedure (for **14c**) with a similar problem: The precipitating powder could be purified through washing with (cyclo)pentane, but it retained some LiBr that was carried over to the fresh solvents and the NMR studies. The alternative performance of this Br/Li interchange reaction directly in Et_2O or *t*-BuOMe at –75 °C was unprofitable since **14d** was generated in competition with formation of a similar amount of the acetylide PhCCLi. In contrast to **14a** and **14b**, the purified samples of **14d** were thermally stable up to 110 °C for at least a few minutes in THF as the solvent. With a sufficient portion of saturated hydrocarbons as cosolvents, such THF solutions remained liquid at and below –118 °C during the ^{1}H and ^{13}C NMR runs that disclosed the presence of both monomeric and dimeric **14d** (Tables S5a[18] and S5b). The monomeric species (entry 10

of Table 1; Figure 1f) was identified through its lithiation shifts $\Delta\delta$ that resembled those of the established monomers of **5a**, **12**, **14a**, and **14b** (entries 1, 3, 5, and 7). Dimeric **14d** was recognized at –118 °C (entry 11) in the same solution through its $\Delta\delta$ data that resembled those of dimeric **14c** (entry 9). The separated ^{1}H and ^{13}C NMR signals of these two **14d** species coalesced pairwise in the temperature region of –104 °C; on further warm-up, the averaged resonance positions moved according to a changing monomer/dimer population ratio: With a total **14d** concentration of 0.3 M in units of the monomer formula, ca. 40% of the material in THF was in the monomeric form at and below –118 °C but only ca. 20% at 25 °C. The ^{1}H NMR spectrum of such a mixture (Figure 2b) exhibited the typical upfield shifts of 4-H (triplet) and 2-/6-H (doublet) that result through delocalization of negative electric charge from the Li–C(α) bond into the aromatic π system (quasi-benzyllithium resonance[8,15]). The monomer population of **14d** in THF was higher than that of **14c** (bearing 4-CH_3) but lower than those of **14b** (4-Cl) and **14a** (4-$SiMe_3$). The dimeric species of **14d** was present also in the solvent *t*-BuOMe, as shown by comparison of the data in entries 11 and 12 or in Figures 1e and 1g; this dimer was accompanied by two unidentified components (but not by monomeric **14d**). These two components (Agg1 and Agg2) were **14d** species since all of their ^{1}H and ^{13}C NMR signals formed weighted averages with those of the dimeric species above the coalescence temperatures of about –50 °C, as shown in Tables S6a[18] and S6b. For instance, the averaged δ values up to 25 °C were roughly compatible with the dimer/Agg1/Agg2 ratio of ca. 3:5:2 that was measured at –118 °C. Figure 2a displays the ^{1}H NMR spectrum of that mixture with δ values that differ substantially from those of the monomer/dimer mixture in Figure 2b. (The broad hump belongs to polymerized material, and the *trans*-H doublet is broadened through a neighbourly magnetic interaction with ^{6}Li.) Replacing the excess portion of the *t*-BuOMe solvent by cyclopentane, we re-encountered with Agg1 as a highly predominant species of **14d** that exhibited practically the same ^{13}C NMR shifts at –80 °C (Table S7a[18]) as in *t*-BuOMe as the solvent. On the other hand, the broadened two-proton NMR resonance of 2-/6-H was peculiarly temperature-dependent (Table S7b[18]), perhaps due to the shortage of *t*-BuOMe (ca. 2.4 equiv) donor ligands in cyclopentane. Nevertheless, the higher than dimeric aggregational state of Agg1 was clearly evident from entry 13 (Table 1) and Figure 1h by the typically[11] diminished $\Delta\delta$ magnitudes of C-α, C-1, C-2/-6, C-3/-5, and C-4. It will be shown in the next section that Agg1 was solvated by d = 1 *t*-BuOMe ligand per carbanion unit at +25, –25, and –41 °C.

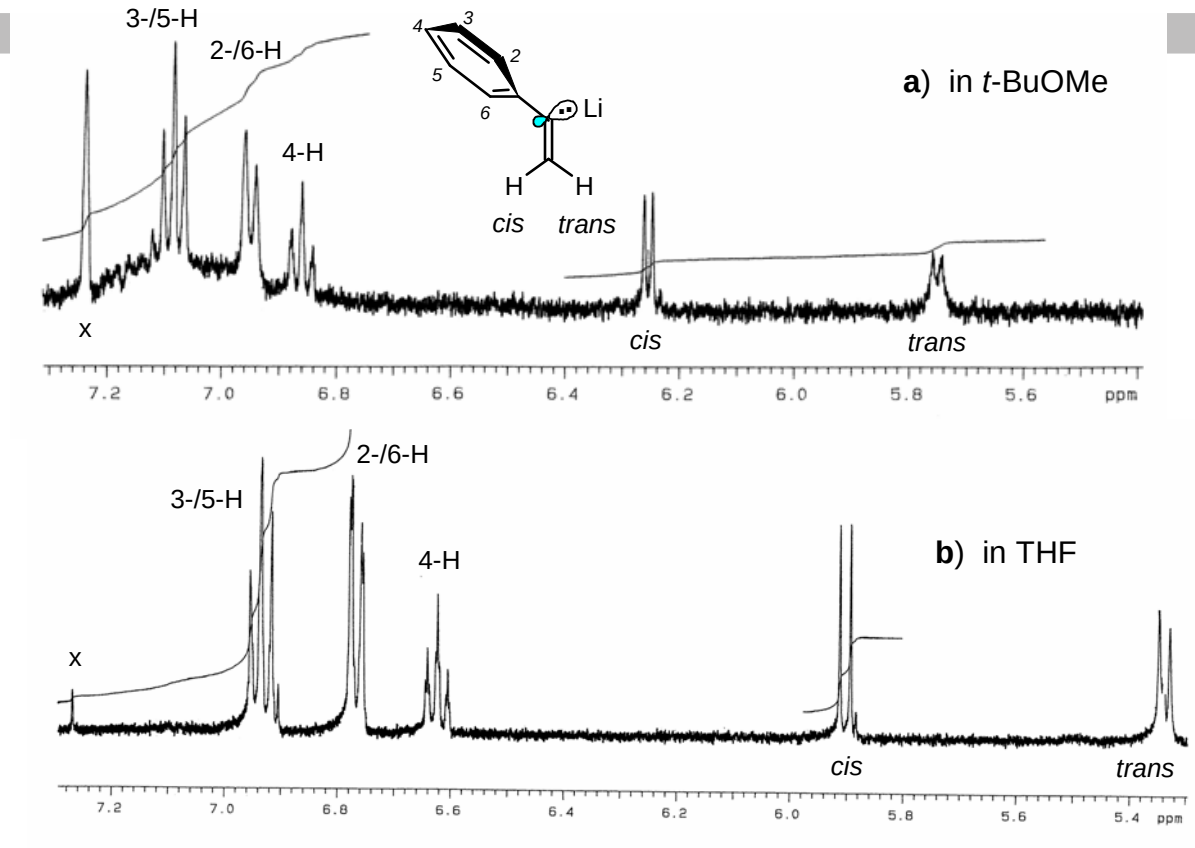

Fig. 2. ^{1}H NMR spectra (400 MHz, 25 °C) of dimeric α-lithiostyrene (**14d**) in rapidly equilibrating mixtures with its congeners: a) averaged with higher **14d** aggregates (ca. 70%) in *t*-BuOMe as the solvent; b) averaged with monomeric **14d** (ca. 20%) in THF; x = benzene.

This section revealed that the α-lithiostyrene family (**14d**) consisted of a least four members, three of which (dimer, Agg1, and Agg2) coexisted in *t*-BuOMe as the solvent, while the monomeric and dimeric species alone were met in THF. A shortage of the donor ligand *t*-BuOMe in cyclopentane favored the preponderant species Agg1. With electron-withdrawing *para*-substituents (4-$SiMe_3$ and 4-Cl), **14a** and **14b** were predominantly monomeric in THF but remained purely dimeric in Et_2O as the solvent; unfortunately, they were inconveniently prone to polymerization. The 4-CH_3 derivative **14c** was (like **10**) one of our first examples with a strong inclination toward dimerization in THF.

2.2. Differentials of $^{2}J_{H,H}$ can disclose microsolvation

Microsolvation numbers *d* of β-unsubstituted vinyllithium derivatives ("RLi") may be recognized by their linear relationship with the two-bond NMR coupling constants $^{2}J_{H,H}$ of the CH_2-β protons: The empirical[11] eq 1 predicted that unsolvated (*d* = 0) samples should display $^{2}J_{H,H}$ = 3.9 Hz, whereas the experimental values were 4.6 Hz[15] for **11** and 4.5 Hz[15] for **12** (Scheme 1). As a possible explanation, "solvation" by the contaminating LiBr (often

ca. 0.3 equiv) in the donor-free solutions may account for these somewhat oversized magnitudes of $^2J_{H,H}$. In fact, this interference by LiBr disappeared in ethereal solvents that solvated both LiBr and the organolithium species separately, so that their THF solutions showed ^{1}H NMR data that equaled those of LiBr-free **14d** in THF.[20] However, the solvation-independent term 3.9 ppm in eq 1 may contain constitutional contributions that are also present in the $^2J_{H,H}$ values of the appertaining "parent" alkenes ("RH"). This was hitherto of little consequence for us as long as $^2J_{H,H}$ magnitudes of RH were hardly different: 2.2 (±0.2) Hz for 2,6-dimethylstyrene[21–23] (= RH of **5a**), 1.7 Hz[15] for RH of **11**, 1.76 Hz[15] for RH of **12**, 1.9 Hz[14] for RH of **8**, and 1.7 Hz[14] for RH of **9**. However, we now have to consider[18] the diminished $^2J_{H,H}$ magnitudes of other alkenes (RH) such as **15a** (1.0 Hz),[24] **15b** (0.87 Hz),[25] **15c** (1.11 Hz),[26] and **15d** (1.09 Hz).[26] Hence, the empirical eq 2 with $^2J_{H,H}$ differentials ($\Delta^2J_{H,H}$)[13] is now proposed as a numerically identical re-formulation of eq 1. The new solvation-independent part [1.7(1) Hz in eq 2] may still contain smaller contributions to $^2J_{H,H}$ from residual constitution- and conformation-dependent effects that are not equal for RLi (**14**) and RH (**15**). For unsolvated **14a** and **14b**, eq 2 (d = 0) predicts $^2J_{H,H}$ = ca. 1.7 + 0.9 ≈ 2.6 Hz, whereas the experimental values were ca. 4 Hz in Section 2.1. Of course, we must allow again for "solvation" by the contaminating LiBr in the "donor-free" hydrocarbon solutions. (**14c** and **14d** were not sufficiently soluble in donor-free, saturated hydrocarbons.) As this LiBr effect vanished in ethereal solvents, as deduced above, eq 2 provided reliable estimates for the microsolvation numbers d in the following examples. Column "d" in Table 1 displays the (numerically over-exact) results before rounding off: The monomeric species are trisolvated (d ≈ 3 in entries 1, 3, 5, and 7), and monomeric **12** (entry 3) appeared to populate its dimeric species at rt in THF. As usual, dimeric **5a** was disolvated (d = 1 *t*-BuOMe ligand in entry 2);[11] hence it came as a surprise that the dimeric *ortho*-unsubstituted α-lithiostyrenes **14a–c** (entries 6, 8, and 9) appeared to be tetrasolvated by d = 2 ligands per carbanion unit, presumably due to facilitated immobilization of a second "explicit" ligand per Li center. Regrettably, $^2J_{H,H}$ coupling was not resolved for the two separated species of **14d** in THF; we therefore took recourse to comparisons of the $\Delta\delta$(C-α) and $\Delta\delta$(C-1) data which suggested that monomeric **14d** was trisolvated (entry 10 compared with 7) and that dimeric **14d** was tetrasolvated in THF (entry 11 compared with 9 and 12). The unidentified higher aggregate Agg1 of **14d** turned out to be solvated by d = 1 *t*-BuOMe ligand in cyclopentane solution (entry 13). Consequently, the mixture of tetrasolvated dimer (d = 2) with the higher aggregated species in *t*-BuOMe should provide averaged d values between 1 and 2 under conditions of rapid interconversion; this prediction agrees with the observed value of d = 1.8 (above –22 °C in entry 12).

$$^2J_{H,H} = d \times 1.67\ \text{Hz} + 3.9\ \text{Hz} \quad (1)$$

$$\Delta(^2J_{H,H}) = {}^2J_{H,H}(\text{RLi}) - {}^2J_{H,H}(\text{RH}) = d \times 1.67\ \text{Hz} + 1.7(1)\ \text{Hz} \quad (2)$$

Hexamethylphosphoramide (HMPA) is known to coordinate much more strongly than THF to Li cations.[27] Thus, a modest concentration of HMPA (1.1 M, ca. 2 equiv) sufficed apparently to shift the mobile monomer/dimer equilibrium (ca. 1:4) of **14d** in THF at rt toward the trisolvated monomer with $^2J_{H,H}$ = 8.0 Hz (formally d = 3.1 by eq 2). Actually, a somewhat higher portion of HMPA (3 equiv) created the lithiation shift $\Delta\delta$(4-H) = –0.76 ppm for **14d** in THF; this value exceeded the magnitude of $\Delta\delta$(4-H) = –0.61 ppm for **14d** in the absence of HMPA (entry 10, or Figure 1f). This demonstrated that HMPA-solvated Li^+ is more electron-releasing than THF-solvated Li^+, which is understandable because the oxygen atom in HMPA carries a formal negative charge. As a consequence, this reduced electronegativity of HMPA-solvated Li^+ may exaggerate the magnitude of $^2J_{H,H}$ that depends the σ-inductive effect within the double-bond plane, as explained previously.[11] Indeed, still higher HMPA concentrations increased $^2J_{H,H}$ up to at least 8.9 Hz at –74 °C, for which eq 2 would predict an overestimated microsolvation number of d = 3.7; this suggested that eq 2 would require a modified parametrization for counting electrically charged donor centers such as in HMPA or the "solvating" LiBr of Section 2.1. However, such a modification was deemed unnecessary as far as the microsolvation numbers d = 1 – 4 of HMPA could be determined directly through inspection[27] of Li/^{31}P NMR coupling patterns.

This section illustrated the applicability of the empirical eq 2 that infers microsolvation numbers from "differential" two-bond inter-proton coupling constants $\Delta^2J_{H,H}$ of β-unsubstituted vinyllithiums. Experimental problems arose occasionally through serious line broadening of this olefinic =CH_2 AB spectral system in **14**.

2.3. Cis/trans stereoinversion in THF

The pseudomonomolecular, ionic mechanism[8,11] of *cis*/*trans* stereoinversion (Scheme 3) was established for the trisolvated, monomeric species of the alkenyllithiums **1a**–**e**, **2**, **3a**–**b**, **5a**–**c**, **9**, **11**, and **12** in THF as the solvent. It proceeds via an NMR-invisible, solvent-separated ion pair with transitory immobilization of a fourth THF ligand at Li; therefore, it is catalyzed by THF at the expense of a characteristically negative pseudoactivation entropy of $\Delta S_\psi^\ddagger$ = ca. –23(3) cal mol^{-1} K^{-1}. For α-arylvinyllithiums such as **5**, **9**, **11**, or **12**, this stereoinversion interconverted the *cis* and *trans* environments of the two diastereotopic β-H nuclei. Depending on the applied magnetic field strength and the temperatures, increasing rates of this "diastereotopomerization" will first broaden the four-line (AB type, Section 2.2) proton pattern and then lead to coalescence into a singlet signal at the resonance position of

($\delta_A + \delta_B$)/2.[28] Computer-aided total line-shape simulations[29] afforded the pseudo-first-order rate constants k_ψ which depend on the THF concentration and on the Kelvin temperatures *T*. The linear correlation of the logarithms of these k_ψ values (Tables S9–S12[18]) versus 1/*T*, as illustrated by the Arrhenius plots in Figure 3, afforded the pseudoactivation parameters $\Delta G_\psi^\ddagger = \Delta H_\psi^\ddagger - T \times \Delta S_\psi^\ddagger$ for the stereoinversion of **14a**, **b**, and **d** in THF. The predominantly monomeric α-[4-(trimethylsilyl)phenyl]vinyllithium (**14a**, entry 4 of Table 2) could be measured at temperatures up to 62 °C and turned out to be the fastest member of this series (line c of Figure 3, and entries 4–6 of Table 2). The more readily polymerizing α-(4-chlorophenyl)vinyllithium (**14b**) inverted a little less rapidly (Figure 3, line b) and furnished practically the same pseudoactivation entropy $\Delta S_\psi^\ddagger$ as **14a** (entries 4 and 5). Both of these $\Delta S_\psi^\ddagger$ values were significantly more negative than the above-mentioned benchmark of $\Delta S_\psi^\ddagger$ = ca. –23(3) cal mol^{-1} K^{-1} and the values in entries 1 – 3. Since these entropy values are partially due to immobilization of the fourth THF ligand in an ion-pair intermediate, their increased magnitudes in entries 4 and 5 may be understood as a hint at the possiblility that the stereoinversions of **14a** and **14b** (Scheme 3) depended on both the trisolvated monomeric (*d* = 3) and the tetrasolvated dimeric (*d* = 2) species: The transitory immobilization of more than one THF ligand in order to generate $Li^+(THF)_4$ from the dimeric portion would then create an additional entropic penalty. Compared with **5a** (entry 1) and **12** (entry 2), the strongly diminished pseudoactivation enthalpies $\Delta H_\psi^\ddagger$ in entries 4 and 5 were caused partially by the accelerating effect of the *para*-substituents 4-$SiMe_3$ and 4-Cl, respectively, as expected from the following established[8] trait of the ionic stereoinversion mechanism. The appertaining Hammett reaction constant ρ = +5.2 (discovered[8] with **1a**–**e**) is an essential piece of mechanistic evidence; as far as it is applicable also to the α-lithiostyrenes **14a–d**, it would predict for **14d** a $\Delta G_\psi^\ddagger$(0 °C) barrier that should be higher by ca. 1 kcal mol^{-1} than those of the more rapidly inverting **14a** and **14b** (ca. 14.8 kcal mol^{-1} in entries 4 and 5). Such an estimate would approach the barrier of ca. 16.2 kcal mol^{-1} (entries 1 and 2) that could have been expected for **14d** because *ortho*-CH_3 groups do not[14] change the barriers of **5a** (with *ortho*,*ortho´*-dimethyl) and **12** (with one free *ortho*-position). Instead, the observed value (entry 6) was even higher by almost 1.5 kcal mol^{-1}, which suggests to look more closely at the kinetic problems with **14d** in the sequel.

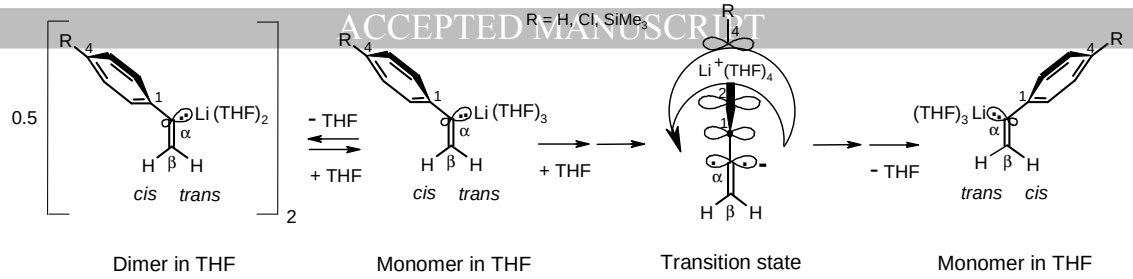

Scheme 3. The rapidly reversible formation of tetrasolvated dimers withdraws fractions of the trisolvated monomers of **14a**, **b**,or **d** from their pseudomonomolecular, ionic *cis*/*trans* stereoinversion process in THF as the solvent.

Table 2. Pseudoactivation parameters $\Delta G_{\psi}^{\ddagger}$ (kcal mol^{-1} at 0 °C), $\Delta H_{\psi}^{\ddagger}$ (kcal mol^{-1}), and $\Delta S_{\psi}^{\ddagger}$ (cal mol^{-1} K^{-1}) for the *cis*/*trans* diastereotopomerization rates of α-arylvinyllithiums **5a**, **9**, **12**, **14a**, **14b**, and **14d** in THF.

entry	compd	aryl group [a]	$\Delta G_{\psi}^{\ddagger}$(0 °C)	$\Delta H_{\psi}^{\ddagger}$	$\Delta S_{\psi}^{\ddagger}$	HT [b]	Ref.
1	**5a**	2,6-Me_2Ph	16.3 (±0.1)	10.2 (±0.7)	–22.2 (±2.2)	+5.0	11
2	**12**	2-MePh	16.14 (±0.05)	10.6 (±0.3)	–20.2 (±0.8)	+74.0	15
3	**9**	naphthyl-1	12.94 (±0.01)	6.9 (±0.1)	–22.3 (±0.4)	+28.0	14
4	**14a**	4-Me_3SiPh	14.57 (±0.05)	6.4 (±0.4)	–29.8 (±1.2)	+62.0	c
5	**14b**	4-ClPh	15.06 (±0.03)	7.3 (±0.4)	–28.3 (±1.3)	+35.5	c
6	**14d** [d]	phenyl	17.68 (±0.05)	7.9 (±0.3)	–35.9 (±1.1)	+80.0	c
7	**14d** [e]	phenyl	13.95 (±0.00)	6.1 (±0.3)	–28.9 (±0.9)	+28.0	c

[a] Me = methyl, Ph = phenyl. [b] HT = highest temperature (°C) of the rate measurements. [c] This work. [d] [**14d**] = 0.6 M. [e] [**14d**] = 0.57 M, [HMPA] = 1.1 M, [LiBr] = 0.7 M, $^2J_{H,H}$ = 8.5 Hz.

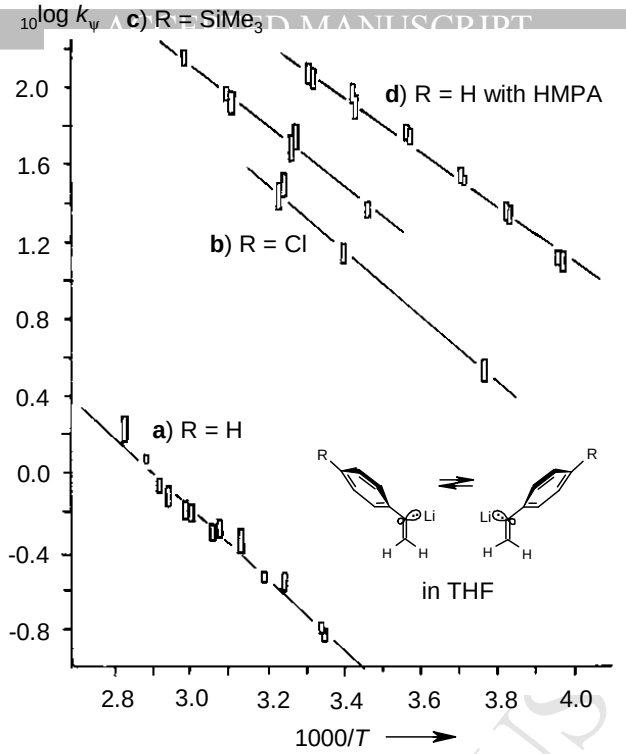

Fig. 3. Temperature-dependent decadic logarithms ($_{10}$log) of the pseudo-first-order stereoinversion rate constants k_ψ (s^{-1}) of the α-lithiostyrenes **14a**, **14b**, and **14d** in THF (Tables S9–S12[18]): (a) **14d**; (b) **14b**; (c) **14a**; (d) **14d** with HMPA (2 equiv).

Our stereoinversion studies with α-lithiostyrene (**14d**) posed the theoretical problem that it would not be possible to obtain detailed knowledge about the individual contributions of the monomeric and dimeric components even though dimeric[22] and higher aggregates are known[11] to invert more slowly (by unidentified mechanisms) than the monomers. Furthermore, experimental confirmations of the above-considered increase of $\Delta G_\psi^{\ddagger}$(0 °C) for **14d** were foreshadowed by the practical problem of measuring stereoinversion rate constants k_ψ that were often not fast enough to generate suitable line-broadening in the lower temperature regions even at NMR machine frequencies as small as 100 or 60 MHz. Therefore, we used also the double-resonance NMR-relaxation technique that was described by Forsén and Hoffman[30a] and improved by Anet and Bourn.[30b] We applied this saturation-transfer method to the equilibrating mixture (47:53) of (*Z*)- and (*E*)-[β-D_1]**14d** that had been prepared from (*E*,*Z*)-[β-D_1]**13d**[18] (Scheme 4). With deuterium decoupling of the two =CHD proton singlets of (*Z*,*E*)-[β-D_1]**14d** in THF, a sudden selective ^{1}H irradiation ("saturation") of the *Z* singlet reduced the intensity of the *E* singlet (or vice versa) at a rate that depended on the $Z \rightarrow E$ (or $E \rightarrow Z$, respectively) stereoinversion rate. For simplicity, we report (Table S11[18]) k_ψ values that are weighted averages of the slightly differing $Z \rightarrow E$ and $E \rightarrow Z$ rate constants (whose ratio accounts for the above equilibrium mixture). The temperature dependence of k_ψ (line a of Figure 3) afforded the pseudoactivation parameters for the

monomer/dimer mixture listed in entry 6 of Table 2: Compared with monomeric **5a** (entry 1), the dimeric fraction of **14d** appeared to have lowered both $\Delta H_{\psi}^{\ddagger}$ (by more than 2 kcal mol^{-1}) and $\Delta S_{\psi}^{\ddagger}$ (by almost 14 units); these trends agree with the usual[17] exothermic and entropy-consuming deaggregation of dimeric α-arylalkenyllithiums in THF.

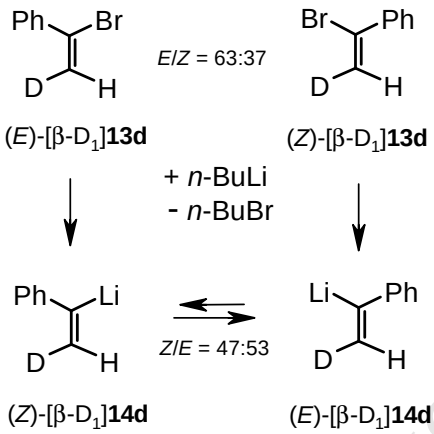

Scheme 4. Preparation and *Z*,*E*-stereoinversion equilibrium of [β-D$_1$]**14d**.

Should we interpret these **14d** properties on the basis of the ionic stereoinversion mechanism that applies to **5a**? Admixtures of dry LiBr to **14d** in THF appeared to cause modest (up to 6-fold) accelerations that resembled those observed[31] for **5a**, whereas additions of dry (aprotic) LiO*t*-Bu did not change the rate-broadened line shapes; this absence of an equal-cation-caused retardation effect agreed with the absence of an ionic dissociation step from the established[8,11] ionic stereoinversion mechanism. On the other hand, additions of increasing portions of aprotic KO*t*-Bu (up to 1 equiv) accelerated not only the stereoinversion dramatically (up to > 200-fold) but also the decomposition of **14d**. Thus, an increased ionic character of the (presumably monomeric) alkenylpotassium compound facilitated the stereoinversion. An even stronger acceleration by almost 3 orders of magnitude can be visualized by comparing the log k_{ψ} data of **14d** in line a of Figure 3 with those in line d of Figure 3 for **14d** in the presence of HMPA (2 equiv). The latter system diastereotopomerized rapidly enough at low temperatures to permit the use of a few line-shape simulations that yielded concordant k_{ψ} values for [β-D$_1$]**14d** and unlabeled **14d** (hence, no perceptible kinetic isotope effect). The pseudoactivation parameters of such a run (entry 7 of Table 2) suggested a twofold effect of HMPA: Compared with entry 6, the further decrease of $\Delta H_{\psi}^{\ddagger}$ may be due to stronger energetic stabilization of both the ion-pair intermediate and the stereoinversion transition state than of the ground state of **14d**. Energetic ground state stabilization by HMPA (2 equiv) was also supposed in Section 2.2 to decrease the dimer population; this second effect can account for the reduced magnitude of $\Delta S_{\psi}^{\ddagger}$ (entry 7) in the direction toward the entropies of the monomers in entries 1–3. Regrettably, an attempted closer approach to the

entropy bench mark values of –23(3) cal mol^{-1} K^{-1} was unattainable because higher HMPA concentrations (> 3 equiv) led to the increasingly rapid decomposition of **14d** and to ill-defined activation parameters.[16] However, the observed pseudoactivation parameters with HMPA (entry 7) appeared to be still compatible with the ionic mechanism.[32]

This section illustrated that an equilibrating system of monomeric and dimeric species of the α-lithiostyrene **14d** can impair numerically more precise interpretations of the kinetic results. Nevertheless, we could demonstrate that **14d** satisfies several criteria for the ionic mechanism: The rate constants k_ψ were higher in THF than in Et_2O or *t*-BuOMe as the solvents; they stayed unchanged with LiO*t*-Bu as an equal-cation additive in THF but were substantially increased by added HMPA ligands or by π-electron-withdrawing *para*-substituents, while a *para*-methyl group in dimeric **14c** retarded the inversion so much that ^{1}H NMR line-broadening could not be detected up to 73 °C in THF. However, all observed k_ψ data were averages of those of the smaller monomeric fraction (≤ 20%) and of the significantly lower rate constants[22] of a major dimeric fraction. As a consequence, k_ψ must decrease when the monomeric population decreases with increasing concentrations of **14d**. Purely monomeric **14d** should invert with the same $\Delta G_\psi^{\ddagger}(0\ °C) \approx 16.2$ kcal mol^{-1} as **5a** and **12**, whereas the experimental value (entry 6) was $\Delta G_\psi^{\ddagger}(0\ °C) = 17.68(5)$ kcal mol^{-1}; the rise by 1.5 kcal mol^{-1} can be ascribed to the presence of dimeric **14d** that participated indirectly in the stereoinversion process through deaggregation.

3. Conclusion

(i) The structural assignments by secondary NMR criteria ($\Delta\delta$ values) and the conclusions in this work were based on ample background knowledge that had been collected from the analytically more suitable systems shown in Scheme 1. The more complicated (because rapidly scrambling) systems of **14d** in THF or *t*-BuOMe might be suited for additional reactivity studies by the Rapid Injection NMR[33] technique.

(ii) In contrast to the purely monomeric nature of α-(2,6-dimethylphenyl)vinyllithium (**5a**) and several other alkenyllithiums (Scheme 1), the *ortho,ortho´*-unsubstituted α-lithiostyrene (**14d**) formed a monomer/dimer mixture (ca. 1:4 at 25 °C in units of the monomer formula) in THF as the solvent. This very mobile dimerization equilibrium required temperatures below –101 °C for detecting and assigning the two components. The equilibrium ratios changed with the nature of the *para*-positioned substituents: The electron-withdrawing 4-$SiMe_3$ and 4-Cl groups preferred an increased monomer population in THF, whereas the electron-repelling 4-CH_3 group tolerated only the dimeric species. Modest portions of HMPA (2–3 equiv) appeared to deaggregate the dimeric species of **14d** in THF.

(iii) In *t*-BuOMe as the solvent, the equilibrating mixture of dimeric **14d** (ca. 30%) and two unidentified aggregates (ca. 50 and 20%) "froze" already below –60 °C and provided no NMR-evidence for the presence of a monomeric species. Only this major, *t*-BuOMe-solvated aggregate was found in cyclopentane as the solvent.[34]

(iv) In analogy with the examples depicted in Scheme 1, the monomeric species of **14a**, **b**, and **d** were detected to be trisolvated in THF. These microsolvation numbers (d = 3) of electrically uncharged donor centers (excluding HMPA) could not be measured through NMR integration; instead, they were calculated from the magnitudes of the $H_2C=$ interproton coupling constants $^2J_{H,H}$ (eq 1) or from the numerically equivalent empirical relationship (eq 2) that uses the difference $\Delta^2J_{H,H} = {}^2J_{H,H}(RLi) - {}^2J_{H,H}(RH) = d \times 1.67$ Hz + 1.7(1) Hz of RLi and its "parent" RH. Unlike all disolvated dimeric *ortho*-substituted examples in Scheme 1, the dimers of the *o,o´*-unsubstituted α-lithiostyrenes **14a**–**d** were found to be tetrasolvated with the microsolvation number d = 2 electron-pair donor ligands per Li. Eq 2 served also to recognize d = 1 *t*-BuOMe ligand per carbanion unit of the preponderant higher aggregate of **14d** in cyclopentane.

(v) The interconversion of the *cis* and *trans* environments of the $H_2C=$ protons of the α-lithiostyrenes **14a**, **b**, and **d** occurred most rapidly in THF as the solvent. In accord with the established pseudomonomolecular, ionic stereoinversion mechanism,[8] the *para*-substituents $SiMe_3$ and Cl accelerated this *cis*/*trans* interconversion, and the absence of *ortho*-substituents did not facilitate this process. Although the very mobile dimerization equilibrium in THF prevented detailed interpretations of the rate constants, their apparent pseudoactivation parameters in Table 2 (entries 4 – 7) were compatible with the ionic mechanism[8] The addition of KO*t*-Bu or HMPA accelerated both the *cis,trans* stereoinversion and the decomposition of **14d** strongly.

(vi) Since the above *cis,trans* stereoinversion mechanism[8] applies to monomeric α-lithiostyrene (**14d**), the pseudoactivation parameters in entry 6 of Table 2 can provide the following answer to the title question. As far as dimeric **14d** in THF is much less stereolabile than the monomer, its rapidly reversible deaggregation lowered $\Delta S_\psi^\ddagger$ (by 13.7 units) more than $\Delta H_\psi^\ddagger$ (by 2.3 kcal mol^{-1}), both relative to purely monomeric **5a** in entry 1. This retardation by an increase of $\Delta\Delta G_\psi^\ddagger(0\ °C) \approx 1.4$ kcal mol^{-1} can be ascribed to the kinetically inactive fraction (namely, dimeric **14d**) that reduced the active monomeric population of **14d**. In short, the stereoinversion rate of the partially monomeric **14d** was accelerated by two *ortho*-methyl groups in **5a** because they made their ground state of **5a** fully monomeric.[35]

4. Experimental

4.1. General information

The previously[7,8,12] described methods were applied to perform the preparations and reactions of organolithium samples in NMR tubes under argon gas cover. All ^{1}H and ^{13}C chemical shifts were referenced to internal Me_4Si; abbreviations for the signal multiplicities are as follows: d = doublet, dd = doublet of doublets, ddt = doublet of doublets of triplets, dm = doublet of multiplets, dtd = doublet of triplets of doublets, m = multiplet, q = quartet, qi = quintet, quat = quaternary, s = singlet, sept = septet, t = triplet. All concentrations and populations were counted in units of the monomer formula.

*4.2. α-Bromo-4-(trimethylsilyl)styrene (**13a**)*

1,1-Dibromo-1-[4´-(trimethylsilyl)phenyl]ethane (388 mg, 1.15 mmol), prepared[18] from 4-(trimethylsilyl)acetophenone,[36] was dissolved in anhydrous *N*,*N*-dimethylformamide (2.5 mL) and heated to 90 °C under dry inert gas for 18 min (method A2 in Ref. 37). The cooled mixture was dissolved in Et_2O (25 mL), washed with distilled water (5 × 6 mL), dried over $MgSO_4$, filtered, concentrated under dry inert gas, and dried for 1 h under reduced pressure at rt. The crude material (290 mg) became oxidized easily on contact with air to give α-bromo-4-(trimethylsilyl)acetophenone (δ_H = 0.30 and 4.20 ppm) that distilled together with the known[38] liquid product **13a** (bp 47 °C/0.005 mbar).

^{1}H NMR of **13a** ($CDCl_3$, 400 MHz) δ 0.27 (s, 9H, Me_3Si), 5.77 and 6.12 (AB spectral system, ^{2}J = 2.0 Hz, 1 + 1H, olefinic CH_2-β), 7.50 and 7.56 (AA´BB´ system, ^{3}J = 8.4 Hz, 2 × 2H, 2-/3-/5-/6-H) ppm;

^{13}C NMR of **13a** ($CDCl_3$, 100.6 MHz) δ –1.2 (qsept, ^{1}J = 119.5 Hz, ^{3}J = 2.0 Hz, Me_3Si), 117.6 (dd, apparent ^{1}J = 167.1 and 158.4 Hz, CH_2-β), 126.5 (ddt, ^{1}J = 159.8 Hz, ^{3}J = 5.2 Hz, apparent ^{4}J = ca. 2 Hz, C-2/-6), 131.1 (pseudo-qi, apparent ^{3}J = 5 Hz, C-α), 133.3 (sharp dd, ^{1}J = 158.5 Hz, ^{3}J = 8.6 Hz, C-3/-5), 138.8 (dtd, ^{3}J = 8.4, 7.8, and 3.6 Hz, C-1), 142.0 (≥ dodecet through ^{3}J to 2-/6-H and the Me_3Si protons, C-4) ppm; assigned through the C,H coupling patterns.

*4.3. α-Bromo-4-chlorostyrene (**13b**)*

The above protocol for **13a** was applied to crude 1,1-dibromo-1-(4´-chlorophenyl)ethane[18] (590 mg, 1.98 mmol) in anhydrous *N*,*N*-dimethylformamide (2.0 mL), yielding ^{1}H-NMR-spectroscpically almost pure **13b**[39] (390 mg, 91%) if kept always under inert gas cover. It became oxidized to α-bromo-4-chloroacetophenone (mp 88–92 °C, δ_H = 4.23 ppm) on contact with air. ^{1}H NMR of **13b** (CCl_4, 80 MHz) δ 5.70 and 6.02 (AB spectral system, ^{2}J = 1.8 Hz,

1 + 1H, olefinic CH_2-β), 7.20 and 7.45 (AA´BB´ system, ^3J = 8.5 Hz, 2 × 2H, 2-/3-/5-/6-H) ppm. This material was dried under reduced pressure of inert gas for the subsequent preparation of **14b**.

*4.4. α-[4-(Trimethylsilyl)phenyl]vinyllithium (**14a**)*

4.4.1. In donor-free pentane. A dry NMR tube (5 mm) was charged with the α-bromoalkene **13a** (47 mg, 0.18 mmol) in pentane (0.5 mL), cooled to –78 °C under argon gas cover, and treated with *n*-Bu^{6}Li (0.18 mmol) in hexane (0.074 mL). After 9 min at 32 °C, the ^{1}H NMR spectra (80 MHz) showed **13a** and the product **14a** in a ca. 45:55 ratio; polymerization began to interfere after 20 min. Nevertheless, the moderately broadened spectrum of **14a** could be analyzed after 15 h at rt despite the presence of its coproduct *n*-BuBr. ^{1}H NMR of **14a** (pentane, 80 MHz) δ 0.18 (s, Me_3Si), 5.54 (d, ^2J = 4.0 Hz, β-H *trans* to α-aryl), 5.97 (d, ^2J = 4.0 Hz, β-H *cis*), 6.66 (d, ^3J = 7.5 Hz, 2-/6-H), 7.24 (d, ^3J = 7.5 Hz, 3-/5-H) ppm.

4.4.2. In Et_2O. A dry NMR tube (5 mm) was charged with the α-bromoalkene **13a** (44 mg, 0.17 mmol) in anhydrous Et_2O (ca. 0.5 mL), cooled to –78 °C under argon gas cover, and treated with *n*-Bu^{6}Li (0.21 mmol) in hexane (0.23 mL). Placed in a large Schlenk tube that was filled with argon gas and held in a tilted position (with a ca. 20° angle above horizontal), the opened NMR tube was cautiously evacuated down to < 0.1 mbar at rt. After venting with dry argon gas, the NMR tube was cooled while its liquid contents were dissolved in anhydrous Et_2O or THF together with 0.060 mL of [D_{12}]cyclohexane.

^{1}H NMR (Et_2O, 400 MHz, 25 °C) δ 0.21 (s, ca. 9H, Me_3Si), 5.64 (broadened, 1H, β-H *trans* to α-aryl), 6.09 (broadened d, ^2J = 5.5 Hz, 1H, β-H *cis*), 6.82 (d, ^3J = 7.5 Hz, 2H, 2-/6-H), 7.23 (d, ^3J = 7.5 Hz, 2H, 3-/5-H) ppm;

^{1}H NMR (THF, 400 MHz, 25 °C) δ 0.17 (s, 9H, Me_3Si), 5.25 (broad d, 1H, β-H *trans* to α-aryl), 5.82 (broadened d, ^2J = 8.0 Hz, 1H, β-H *cis*), 6.71 (d, ^3J = 7.9 Hz, 2H, 2-/6-H), 7.11 (d, ^3J = 7.9 Hz, 2H, 3-/5-H) ppm;

^{13}C NMR (Et_2O, 100.6 MHz, 25 °C) δ –0.6 (Me_3Si), 123.1 (CH_2-β), 124.2 (C-2/-6), 133.7 (C-3/-5), 159.6 (C-1) ppm, C-4 and C-α not detected, assigned through comparison with **14a** in THF;

^{13}C NMR (THF, 100.6 MHz, 25 °C) δ –0.5 (qsept, ^1J = 118.5 Hz, ^3J = 2 Hz, Me_3Si), 117.8 (broadened t, ^1J = 145 Hz, CH_2-β), 123.2 (dd, ^1J = 154 Hz, ^3J = ca. 6 Hz, C-2/-6), 128.1 (quat, C-4), 132.7 (dm, ^1J = 151 Hz, ^3J = ca. 8 Hz, C-3/-5), 164.7 (quat, C-1), 207.1 (quat, C-α) ppm, assigned through the C,H coupling constants and comparison with **1e**.

*4.5. α-(4-Chlorophenyl)vinyllithium (**14b**)*

The above protocol for **14a** was used to generate **14b** in Et_2O solution from α-bromoalkene **13b** and *n*-Bu^{6}Li, followed by evaporation of *n*-BuBr together with all other volatiles. The remaining liquid **14b** and the accompanying LiBr were dissolved in either anhydrous Et_2O or THF.

^{1}H NMR (Et_2O, 400 MHz, 25 °C) δ 5.69 (broadened d, ^2J = 5.8 Hz, 1H, β-H *trans* to α-aryl), 6.11 (d, ^2J = 5.8 Hz, 1H, β-H *cis*), 6.86 (d, ^3J = 8.4 Hz, 2H, 2-/6-H), 7.03 (d, ^3J = 8.4 Hz, 2H, 3-/5-H) ppm, assigned through comparison with **14a**;

^{1}H NMR (THF, 400 MHz, –44 °C) δ 5.12 (d, ^2J = 8.0 Hz, 1H, β-H *trans* to α-aryl), 5.72 (d, ^2J = 8.0 Hz, 1H, β-H *cis*), 6.61 (d, ^3J = 8.4 Hz, 2H, 2-/6-H), 6.86 (d, ^3J = 8.4 Hz, 2H, 3-/5-H) ppm, assigned as above;

^{13}C NMR (Et_2O, 100.6 MHz, 25 °C) δ 124.3 (broadened t, ^1J = 146 Hz, CH_2-β), 126.1 (dd, ^1J = 158.5 Hz, ^3J = 6.8 Hz, C-2/-6), 128.3 (dd, ^1J = 163.0 Hz, ^3J = 4.7 Hz, C-3/-5), 128.5 (quat, C-4), 157.6 (quat, C-1), 199.4 (broad, C-α) ppm, assigned through the C,H coupling constants (especially those of C-3/-5);

^{13}C NMR (THF, 100.6 MHz, –44 °C) δ 117.1 (dd, apparent ^1J = ca. 152 and 138 Hz, CH_2-β), 124.0 (broadened t, ^3J = 10.5 Hz, C-4), 124.5 (sharp dd, ^1J = 156 Hz, ^3J = 6.8 Hz, C-2/-6), 127.1 (dm, ^1J = 159 Hz, C-3/-5), 163.3 (quat, C-1), 207.4 (broadened, C-α) ppm, assigned as above (especially for C-4) and comparison with **14a**.

*4.6. α-(4-Methylphenyl)vinyllithium (**14c**)*

A stirred solution of α-bromo-4-methylstyrene (**13c**, 890 mg, 4.51 mmol) in pentane (2.0 mL) was cooled to –78 °C under argon gas cover and treated with *n*-Bu^{6}Li (5.4 mmol) in isopentane (2.1 mL). This Br/Li interchange reaction proceeded smoothly during the first 5 min and was complete within 60 min at rt. Without delay, the precipitated powder of **14c** was washed with pentane, then dried through evacuation down to < 0.1 Torr, vented with dry argon gas, and dissolved in anhydrous THF. After the NMR studies and later aqueous work-up of the colored solution, a potentiometric titration indicated that the sample had contained 0.23 mmol of LiBr (0.13 equiv).

^{1}H NMR (THF, 400 MHz, 25 °C) δ 2.18 (s, 3H, 4-CH_3), 5.34 (d, ^2J = 7.5 Hz, 1H, β-H *trans* to α-aryl), 5.85 (d, ^2J = 7.5 Hz, 1H, β-H *cis*), 6.65 (d, ^3J = 8.0 Hz, 2H, 2-/6-H), 6.71 (d, ^3J = 8.0 Hz, 2H, 3-/5-H) ppm, assigned through comparison with **14a**;

^{13}C NMR (THF, 25.2 MHz, –44 °C) δ 21.1 (q, ^1J = 126 Hz, 4-CH_3), 118.4 (dd, apparent ^1J = 146 and 136 Hz, CH_2-β), 124.1 (dd, ^1J = 155 Hz, ^3J = 4.5 Hz, C-2/-6), 127.7 (broadened d, ^1J = 151 Hz, C-3/-5 with unresolved ^3J couplings to CH_3 and 5-/3-H), 127.7 (broadened m, apprent J = ca. 5 Hz, C-4), 160.3 (quat, C-1), 206.2 (quat, C-α) ppm, assigned through the C,H coupling patterns.

*4.7. α-Lithiostyrene (**14d**)*

α-Bromostyrene (**13d**, 150 mg, 0.82 mmol) and cyclopentane (0.10 mL) were placed in a dry NMR tube (5 mm) under argon gas cover, cooled to –60 °C, and treated with *n*-Bu^{6}Li (0.85 mmol) in cyclopentane (0.94 mL). After up to 15 h at rt, the colorless precipitate of **14d** and some LiBr was washed with dry cyclopentane (3 × 0.3 mL), then cooled to –30 °C and dissolved in either anhydrous THF or *t*-BuOMe. **Caution:** Dry **14d** may decompose exothermically in contact with only a trace of air! Therefore, it should **not** be stored under a *reduced* pressure of an inert gas.

^{1}H NMR (THF, 400 MHz, 25 °C, Figure 2b) δ 5.34 (d, ^{2}J = 7.5 Hz, 1H, β-H *trans* to α-aryl), 5.90 (d, ^{2}J = 7.5 Hz, 1H, β-H *cis*), 6.62 (tt, ^{3}J = 7.5 Hz, 1H, 4-H), 6.77 (dm, ^{3}J = 7.5 Hz, 2H, 2-/6-H), 6.94 (t, ^{3}J = 7.5 Hz, 2H, 3-/5-H) ppm, assigned through HOESY correlation of ^{6}Li with 2-/6-H and β-H *trans*;

^{1}H NMR (*t*-BuOMe, 400 MHz, 25 °C, Figure 2a) δ 5.70 (d, ^{2}J = 5.8 Hz, 1H, β-H *trans* to α-aryl), 6.16 (sharp d, ^{2}J = 5.8 Hz, 1H, β-H *cis*), 6.80 (tt, ^{3}J = 7.5 Hz, 1H, 4-H), 6.86 (d, ^{3}J = 7.5 Hz, 2H, 2-/6-H), 7.02 (t, ^{3}J = 7.5 Hz, 2H, 3-/5-H) ppm, assigned as above;

^{1}H NMR (cyclopentane with 2.4 equiv of *t*-BuOMe, 400 MHz, 25 °C) δ 5.96 (broad, 1H, β-H *trans* to α-aryl), 6.19 (broadened d, ^{2}J = 4.8 Hz, 1H, β-H *cis*), 6.63 (broadened d, 2H, 2-/6-H), 6.80 (t, ^{3}J = 7.3 Hz, 1H, 4-H), 6.91 (m, 2H, 3-/5-H) ppm, assigned as above;

^{1}H NMR (THF, 60 MHz, –17 °C) of **14d** with HMPA (0.47 M, 3 equiv) δ 6.39 (4-H), 6.55 (2-/6-H), 6.75 (3-/5-H) ppm, assigned through spectral simulation (Figure S6).[18] The olefinic AB spectum was already in coalescence at this temperature and magnetic field strength, showing a very broad resonance centered at δ = 5.33 ppm;

^{13}C NMR (THF, 100.6 MHz, 25 °C) δ 119.5 (t, ^{1}J = ca. 144 Hz, CH_2-β), 120.3 (dt, ^{1}J = 156 Hz, ^{3}J = 7.5 Hz, C-4), 123.9 (dt, ^{1}J = 156 Hz, ^{3}J = 7 Hz, C-2/-6), 127.5 (dd, ^{1}J = 155 Hz, ^{3}J = 7.6 Hz, C-3/-5), 163.1 (ill-resolved m, apparent ^{3}J = ca. 6 Hz, C-1), 205.6 (obscured t, C-α) ppm, assigned through the C,H coupling patterns;

^{13}C NMR (*t*-BuOMe, 100.6 MHz, 25 °C) δ 122.6 (dt, ^{1}J = 155.8 Hz, C-4), 123.2 (broadened t, ^{1}J = 146 Hz, CH_2-β), 124.8 (dt, ^{1}J = 155.7 Hz, ^{3}J = 7 Hz, C-2/-6), 128.1 (dm, ^{1}J = 156 Hz, C-3/-5), 157.8 (unresolved m, C-1), 199.7 (broad, C-α) ppm, assigned as above;

^{13}C NMR (cyclopentane with 2.4 equiv of *t*-BuOMe, 100.6 MHz, 25 °C) δ 123.4 (dt, ^{1}J = ca. 160 Hz, ^{3}J = 7 Hz, C-4), 124.9 (dm, ^{1}J = 158 Hz, C-2/-6), 126.9 (observed at and below –25 °C, CH_2-β), 128.9 (dd, ^{1}J = 155 Hz, ^{3}J = 8 Hz, C-3/-5), 156.7 (unresolved m, C-1), 196.2 (unresolved, C-α) ppm, but C-α at 194.0 ppm/–41 °C, assigned through the C,H coupling constants.

*4.8. α-[4-(Trimethylsilyl)phenyl]acrylic acid (**16a**)*

A solution of the α-bromoalkene **13a** (170 mg, 0.67 mmol) in anhydrous Et_2O (2.5 mL) was cooled to –65 °C, treated with *n*-BuLi (0.67 mmol) in hexane (0.27 mL), and after 1 h at –65 °C poured onto solid CO_2. The warmed-up mixture was dissolved in Et_2O (40 mL) and aqueous NaOH (2 M, 15 mL); the Et_2O layer was extracted with aqueous NaOH (2 M, 4 × 15 mL) and set aside. The combined aqueous extracts were acidified with conc. HCl and shaken with Et_2O (4 × 20 mL). These Et_2O extracts were combined, washed with distilled water (2 × 20 mL), dried over $MgSO_4$, filtered, and evaporated to give the crude acid **16a** (39 mg). The above first Et_2O layer was washed with distilled water until neutral, dried over $MgSO_4$, filtered, and concentrated to yield a mixture (61 mg) of the "parent" alkene **15a** (ca. 45%) and polymerized material. Analytically pure **16a** was obtained through recrystallization from high-boiling petroleum ether (2 ×) and had mp ca. 114 °C.

^{1}H NMR ($CDCl_3$, 400 MHz) δ 0.27 (s, 9H, Me_3Si), 6.03 and 6.54 (AB spectral system, ^2J = 1.1 Hz, 1 + 1H, 2 × β-H), 7.42 and 7.53 (AA´BB´ system, ^3J = 8.2 Hz, 2 + 2H, 2-/3-/5-/6-H), 10.4 (s, 1H, CO_2H) ppm;

^{13}C NMR ($CDCl_3$, 100.6 MHz) δ –1.2 (qsept, ^1J = 119.2 Hz, ^3J = 2.1 Hz, Me_3Si), 127.7 (dd, ^1J = 159.8 Hz, ^3J = 6.1 Hz, C-2/-6), 129.4 (dd, apparent ^1J = 163.6 and 160.2 Hz, CH_2-β), 133.2 (dd, ^1J = 158.3 Hz, ^3J = 8.7 Hz, C-3/-5), 136.4 (broad m, C-1), 140.62 (narrow m, C-α), 140.84 (broad m, C-4), 172.0 (dd, ^3J = 12.5 and 6.5 Hz, CO_2H) ppm, assigned through the C,H coupling constants and comparison with the alkene **15a**;

IR (KBr) ν 3300–2800 (broad O–H), 2956, 1700, 1680 (s), 1251, 1226, 1077, 843, 827 cm^{-1}. Anal Calcd for $C_{12}H_{16}O_2$ (220.3): C, 65.41; H, 7.32. Found: C, 65.82; H, 7.27.

Appendix A. Supplementary Data

NMR data of the styrenes **15a-d** and the acid **16c**; α-bromostyrenes **13a,b** via 1-aryl-1,1-dibromoethanes; deuteriated α-bromostyrenes (*E*)- and (*Z*)-[β-D_1]**14d**; dialkyl ketone adducts **S8**–**S10**; LiBr-free **14d**; tabulated primary NMR data (Tables S1a – S7b); simulations of some ^{1}H NMR spectra of **14d** (Table S8); Rate Measurements (Tables S9–S12).

5. References

1. a) *Lithium Compounds in Organic Synthesis – From Fundamentals to Applications*, Luisi, R., Capriati, V., Eds, Wiley-VCH, 2014;
   b) Capriati V, Perna FM, Salomone A. *J Chem Soc. Dalton Trans.* 2014;43:14204–14210.

2. Reich HJ. *Chem Rev.* 2013;113:7130–7178.
3. Gawley RE. *Topics Stereochem.* 2010;26:93–133.
4. Gessner VH, Däschlein C, Strohmann C. *Chem Eur J.* 2009;15:3320–3334.
5. a) *Lithium Chemistry*, Sapse, A-M, Schleyer, PvonR. Eds. Wiley: New York, 1995; b) Lambert C, Schleyer PvonR. *Angew Chem.* 1994;106:1187–1199; *Angew Chem Int Ed.* 1994;33:1129–1140.
6. For a recent, improved method of determining molecular weights with deviations down to 9% through diffusion-ordered NMR spectroscopy (DOSY), see: Neufeld, R, Stalke D. *Chem Sci.* 2015;6:3354–3364.
7. Knorr R, Menke T, Ferchland K, Mehlstäubl J, Stephenson DS. *J Am Chem Soc.* 2008;130:14179–14188.
8. Knorr R, Menke T, Behringer C, Ferchland K, Mehlstäubl J, Lattke E. *Organometallics.* **2013**, *32*, 4070–4081.
9. Knorr R, Hennig K-O, Böhrer P, Schubert B. *J Organomet Chem.* 2014;767:125–135.
10. Knorr R, Behringer C, Knittl M, von Roman U, Lattke E. *J Am Chem Soc.* 2017;139:4690–4703.
11. Knorr R, Behringer C, Lattke E, von Roman U, Knittl M. *J Org Chem.* 2015;80:6313–6323.
12. Knorr R, Ruhdorfer J, Böhrer P. *Organometallics.* 2015;34:1038–1045.
13. Knorr R, Knittl M, Rossmann EC. *Beilstein J Org Chem.* 2014;10:2521–2530.
14. Knorr R, Behringer C, Ruhdorfer J, von Roman U, Lattke E, Böhrer P. *Chem Eur J.* 2017;23:12861–12869.
15. Knorr R, Lattke E, Ruhdorfer J, von Roman U, Firl J, Böhrer P. *J Organomet Chem.* 2016;824:61–72.
16. Knorr R, Lattke E. *Tetrahedron Lett.* 1977;18:3969–3972, line 7 of Table 1 therein.
17. Knorr, R.; Menke, T.; Ferchland, K. *Organometallics* **2013**, *32*, 468–472, Table 1 therein.
18. See the Supplementary Data.
19. Knorr R, Knittl M, Behringer C, Ruhdorfer J, Böhrer P. *J Org Chem.* 2017;82:2843–2854.
20. Section 5.1 in the Supplementary Data.
21. Gurudata, Stothers JB, Talman JD. *Can J Chem.* 1967;45:731–737. Table 1 therein.
22. Knorr R, Behringer C, Nöth H, Schmidt M, Lattke E, Räpple E. *Chem Ber/Recueil.* 1997;130:585–592.
23. Wright JA, Gaunt MJ, Spencer JB. *Chem Eur J.* 2006;12:949–955, compound **1d** therein.

24. Reynolds WF, Hamer GK, Bassindale AR. *J Chem Soc Perkin Trans 2.* 1977:971–974, Table 1 therein.
25. Hamer GK, Peat IR, Reynolds WF. *Can J Chem.* 1973;51:897–914.
26. Reynolds WF, Peat IR, Hamer GK. *Can J Chem.* 1974;52:3415–3423.
27. For a short NMR desciptin of HMPA-solvated organolithiums, see Figure 1 in: Reich HJ, Kulicke KJ. *J Am Chem Soc.* 1996;118:273–274, and literature quoted therein.
28. An illustration may be found in Ref. 12.
29. For this method and some relevant literature quotations, see Ref. 13.
30. a) Forsén S, Hoffman RA. *J Chem Phys.* 1963;39:2892–2901;
    b) Anet FAL, Bourn AJR. *J Am Chem Soc.* 1967;89:760–768.
31. Figure 2 of Ref. 11.
32. Studies of some other (mostly unsettled) stereoinversion mechanisms under different conditions may be found via the following publications: a) Ref. 22; b) Ref. 11 (Section C and Ref. 19 therein); c) Ref. 8 (Refs. 1–3 and 26–29 therein).
33. For some literature quotations, see Ref. 19.
34. An impressive example of solvent-dependent (THF versus toluene), stereospecifically divergent reactions of a lithiated aziridine was reported by: de Ceglia MC, Musio B, Affortunato F, Moliterni A, Altomare A, Florio S, Luisi R. *Chem Eur J.* 2011;17:286–296.
35. A superficially similar *ortho*-methyl effect prevented a lithiated azetidine from forming a self-coupled (quasi-dimeric) intermediate and derivative; see: Parisi G, Capitanelli E, Pierro A, Romanazzi G, Clarkson GJ, Degennaro L, Luisi R. *Chem Commun.* 2015;51:15588–15591.
36. Eaton C, Ghose BN, Walton DRM. *J Organomet Chem.* 1974;65:169–179, on p 176 therein.
37. von Roman U, Ruhdorfer J, Knorr R. *Synthesis.* 1993;1993:985–992, and quoted literature.
38. Wu J, Yoshika N. *Angew Chem Int Ed.* 2016;55:336–340, compound **1c** on p S2 in the Supporting Information thereof.
39. Gassman PG, Harrington CF. *J Org Chem.* 1984;49:2258–2278, compound **24d** on p 2268 therein.

Scheme 1. α-Arylalkenyllithiums whose (non)aggregation and microsooation states had been established in solution: **1a–e**,[7,8] **2**,[8] **3**,[9] **4**,[10] **5a**,[11] **5b**,[12] **5c**,[13] **6a** and **b**,[10] **7a**,[11] **7b**,[13] **8**,[14] **9**,[14] and **10–12**.[15]

Scheme 2. Preparation and derivatization of the α-arylvinyllithiums **14a–d**.

Scheme 3. The rapidly reversible formation of tetrasolvated dimers withdraws fractions of the trisolvated monomers of **14a**, **b**,or **d** from their pseudomonomolecular, ionic *cis*/*trans* stereoinversion process in THF as the solvent.

Scheme 4. Preparation and *Z*,*E*-stereoinversion equilibrium of [β-D_1]**14d**.

Fig. 1. Lithiation ^{1}H (in parentheses) and ^{13}C NMR shifts $\Delta\delta = \delta(\text{RLi}) - \delta(\text{RH})$ of **14a–d**.

Fig. 2. ^{1}H NMR spectra (400 MHz, 25 °C) of dimeric α-lithiostyrene (**14d**) in rapidly equilibrating mixtures with its congeners: a) averaged with higher **14d** aggregates (ca. 70%) in *t*-BuOMe as the solvent; b) averaged with monomeric **14d** (ca. 20%) in THF; x = benzene.

Fig. 3. Temperature-dependent decadic logarithms ($_{10}$log) of the pseudo-first-order stereoinversion rate constants k_ψ (s^{-1}) of the α-lithiostyrenes **14a**, **14b**, and **14d** in THF (Tables S9–S12[18]): (a) **14d**; (b) **14b**; (c) **14a**; (d) **14d** with HMPA (2 equiv).

Table 1. Microsolvation numbers *d*, NMR coupling constants $^{2}J_{H,H}$ [Hz] of CH_2-β, and lithiation shifts $\Delta\delta = \delta(\text{RLi}) - \delta(\text{RH})$ of the α-arylvinyllithiums **5a**, **12**, and **14a–d** in four solvents.

Table 2. Pseudoactivation parameters $\Delta G_\psi^{\ddagger}$ (kcal mol^{-1} at 0 °C), $\Delta H_\psi^{\ddagger}$ (kcal mol^{-1}), and $\Delta S_\psi^{\ddagger}$ (cal mol^{-1} K^{-1}) for the *cis*/*trans* diastereotopomerization rates of α-arylvinyllithiums **5a**, **9**, **12**, **14a**, **14b**, and **14d** in THF.

* * *

This research did not receive any specific grants from funding agencies in the public, commercial, or not-for-profit sectors.